4th URSI AT-RASC, Gran Canaria, 19-24 May 2024

A Preliminary Indoor Assessment of a Sub-THz Channel Characterizations between 500 GHz and 750 GHz

Qi Li * (1), (2), Ben Chen (3), Ke Guan (3), (4), Lawrence Carslake (2), Yuan Yao (1), and Tian Hong Loh (2)
(1) Beijing University of Posts and Telecommunications, Beijing, China
(2) National Physical Laboratory, Teddington, United Kingdom
(3) School of Electronic and Information Engineering, Beijing Jiaotong University, Beijing 100044, China
(4) State Key Laboratory of Advanced Rail Autonomous Operation, Beijing Jiaotong University, Beijing 100044, China

Abstract

The sub-THz frequency has sparked significant interest in characterizing wireless radio propagation channels beyond 5G communications. However, there is limited research and experimental verification on wide bandwidth propagation channel characteristics in the open literature. This study focuses on modeling and simulating indoor channel scenarios within the 500 GHz – 750 GHz sub-terahertz (sub-THz) frequency band to enhance our understanding of these frequencies' channel characteristics. We validated the simulation platform's accuracy by comparing its results with measured data, confirming its reliability. Using directional horn antennas, we investigated obstructed and unobstructed indoor environments to understand channel behavior at varying distances between transmitting (Tx) and receiving (Rx) antennas within the 500 GHz – 750 GHz frequency band. This work establishes a strong foundation for further research and applications, significantly contributing to our understanding of propagation characteristics in indoor channels within this frequency range.

1. Introduction

Terahertz (THz) and sub-terahertz (sub-THz) waves, positioned between microwave and infrared waves, have promising applications in communication, imaging, sensing. Channel assessment is crucial for designing and optimizing communication systems in this frequency band due to the direct impact of channel characteristics on performance and reliability. Wireless propagation channel assessment involves analyzing signal influences during propagation. The complexity of the sub-THz channel significantly increases due to electromagnetic wave propagation characteristic and atmospheric absorption.

Utilizing diverse simulation platforms is an efficacious approach for in-depth investigation of sub-THz channel characteristics. Through simulations, researchers can emulate the wireless transmission under various channel conditions and capture influential factors such as signal attenuation, multipath propagation, and phase distortion. This facilitates a profound comprehension of the sub-THz channel's attributes and furnishes fundamental data for system design. Reference [1] combines RT and artificial intelligent (AI) algorithms to develop a multi-spectrum propagation model for sixth-generation (6G) wireless technologies, enhancing accuracy and reducing computation time. Reference [2] introduces a super-resolution model using multitask learning Convolutional Neural Networks (CNNs), demonstrating effective recovery of high-resolution channel characteristics in 6G wireless mobile systems, potentially reducing workload in wireless applications. Reference [3] presents a three-dimensional scattering model for accurate THz wave scattering on rough surfaces, providing insights distinct from the existing 3rd Generation Partnership Project (3GPP) channel models and applications in holographic radios and multi-user MIMO (MU-MIMO) systems. In [4], a RTA-SCM for accurate THz V2I communication modeling at 300 GHz is validated against ray-tracing data and stochastic models, offering potential for time-varying THz V2I applications. Reference [5] characterizes the THz band channel for smart rail mobility using ultra-wideband (UWB) channel sounding and RT at 300 GHz, providing valuable insights for THz-enabled Smart Rail Mobility design in the context of 6G. Lastly, [6] characterizes intra-wagon millimeter wave (mm-wave) and sub-mm-wave channels for "smart rail mobility" through UWB channel sounding and RT, offering insights for achieving high-data rate wireless connectivity in smart rail systems. The current research focuses on frequencies below 500 GHz, while the sub-THz band of 500 GHz – 750 GHz still requires extensive simulations and measurements to accurately assess its channel characteristics.

In this paper, we utilize RT technique to modeling and simulate indoor short-distance channel scenario and conduct actual measurements in the 500 GHz – 750 GHz range. The measured results are consistent with the simulation results. Based on verifying the effectiveness of the simulation method, complex indoor long-distance channel scenario is modeled and simulated. Our research providing an important reference for the optimization of communication systems in the sub-THz band.

2. Validation

2.1 Modeling and Simulation

The indoor scenario model presented in Figure 1 is a faithful reproduction of a room at the National Physical

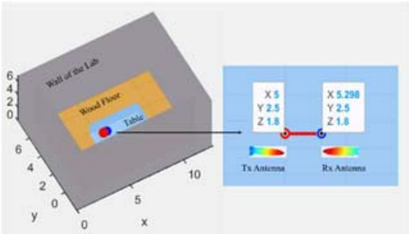

Figure 1. Simulated indoor scenario (taking the distance between the Tx and Rx antenna as 250 mm for illustration purposes)

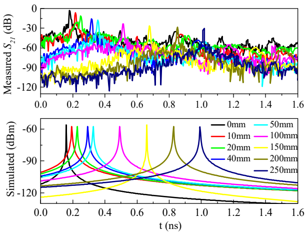

Figure 2. Results of simulated and measured indoor scenario

Table 1. The comparison LOS peak position of ideal, simulated and measured results

Distance (nm)	Ideal Result (ns)	Simulated Result (ns)	Measured Result (ns)	Difference (ns)
0	0.160	0.160	0.180	0.020
10	0.193	0.192	0.216	0.024
20	0.227	0.228	0.248	0.020
40	0.293	0.292	0.316	0.024
50	0.327	0.328	0.356	0.028
100	0.493	0.49a2	0.512	0.020
150	0.660	0.660	0.676	0.016
200	0.827	0.828	0.852	0.024
250	0.993	0.992	1.020	0.028

Laboratory, where channel sounding measurements were conducted. The materials employed in this scenario include wood flooring, brick walls, and a corkboard table. Both the transmitting (Tx) and receiving (Rx) antennas adopt horn antennas with a directivity of 26 dBi and a half power beam angle (HPBA) of 10 degrees. The Tx and Rx antennas are positioned in a straight line, directly facing each other on the table, with separations of 0, 10, 20, 40, 50, 100, 150, 200 and 250 mm. The simulation is conducted using the RT simulation platform. For clarity, in Figure 1, the distance between the transmitting (Tx) antenna and receiving (Rx) antenna is exemplified as 250 mm; however, it should be noted that during simulations, the dimensions of both horn antennas must be taken into consideration.

2.2 Results

The results of the simulated and measured indoor scenario at 500 GHz – 750 GHz is demonstrated in Figure 2. Furthermore, a comparison between the ideal, simulated and measured results of the line-of sight (LOS) peak is presented in Table 1. The simulated LOS peak position closely aligns with the ideal LOS peak position; however, there exists a slight time difference of approximately 0.02 ns between the simulated and measured results. This discrepancy can be attributed to factors such as the waveguide connection flange between the Tx or Rx antenna and frequency extender head, which introduces a distance error of around 6 mm. Additionally, the disparity is further influenced by potential measurement errors in determining the distance between Tx and Rx antennas, as well as calibration error or drift in real measurements. As for increasing distances between Tx and Rx, it is observed

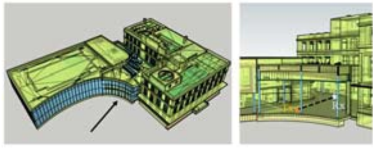

Figure 3. Overall indoor scenario of the evaluated building and specific position of Tx and Rx antenna

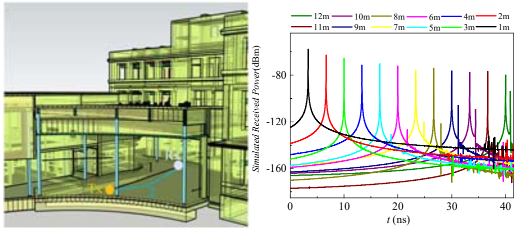

(a) (b)

Figure 4. (a) Ray-tracing simulated 3D path-with horn antenna (b) Ray-tracing simulated results

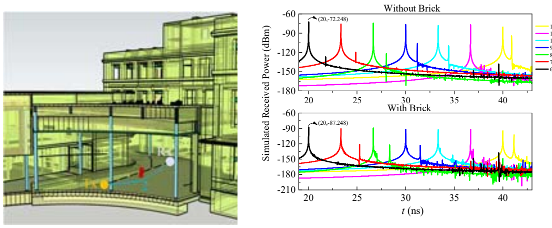

(a) (b)

Figure 5. (a) Ray-tracing simulated 3D path-with brick (b) Ray-tracing simulated results

that there is a minimal change in the simulated peak amplitude due to utilizing ideal materials suitable for low frequencies in this simulation study. However, according to [10], material losses increases with frequency increase; hence, in our measured results, an increase in distance leads to a decrease in LOS peak amplitude. In summary, both simulated and measured outcomes exhibit good agreement overall. Leveraging real-time RT simulation platform enables accurate prediction of THz channel characteristics while providing valuable insights for optimizing communication systems operating within this THz band.

3. Preliminary Indoor Assessment

3.1 Indoor Assessment-without Brick

The overall indoor scenario of the evaluated building and specific positions of the Tx and Rx antenna are illustrated in Figure 3. Modeling and simulation of 500 GHz – 750 GHz were conducted within the evaluated building, using material parameters all sourced from [10] specifically for the THz frequency band, ensuring a more realistic simulation. Figure 4 presents a 3D scene and the RT simulation results as the distance between the Tx and Rx antennas increases. In this scenario, while still employing the same horn antennas, Figure 4 (b) demonstrates that with an increasing distance between the transmitting and receiving antennas, Path1's peak magnitude diminishes while a more prominent reflection path (Path2) emerges (Note: Since reflection or scattering paths below a certain threshold are not displayed in the simulation, only a strong reflection path is captured in this process).

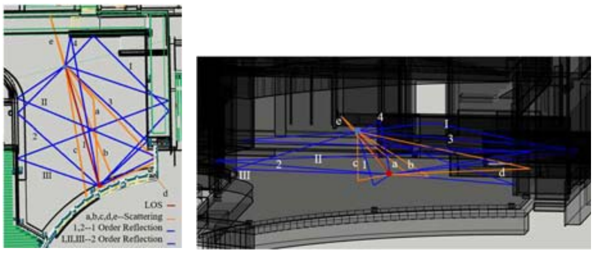

(a) (b)

Figure 6. (a) top view and (b) front view of the evaluated building and corresponding traces (Tx and Rx 12 m)

Table 2. The summary of Paths in Figure 8

Path (m)	1	2	3	4	I	II
Path length (m)	12.2784	16.6298	16.7051	17.6171	23.532	25.3689
τ (ns)	40.928	55.4326	55.6837	58.7237	78.44	84.5631
Path (m)	III	a	b	c	d	e
Path length (m)	32.8546	12.8484	14.1824	15.3149	18.2569	22.0762
τ (ns)	109.5155	42.828	47.2746	51.0498	60.8564	73.5874

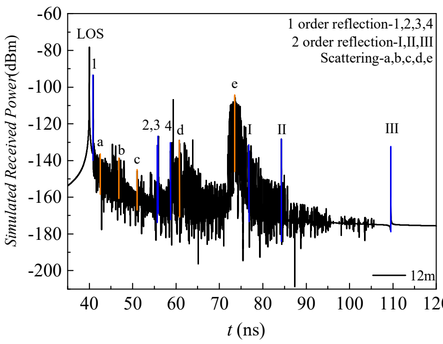

Figure 7. Ray-tracing simulated result

3.2 Indoor Assessment-with Brick

To better predict the channel characteristics of 500 GHz – 750 GHz non-LOS indoor scenarios, modeling and simulation was conducted with an obstruction between the Tx and Rx antennas. First, we still employed horn antennas as both the Tx and Rx antennas, with a separation distance of 12 m. A 1 m×1 m brick was placed at the midpoint of the Rx and the Tx antennas to create an obstruction, gradually reducing their distance to 6 m (as further reduction is not possible due to the brick being at the midpoint). Figure 6 illustrates the corresponding simulation scenario results along with comparison results obtained with and without obstruction present. When a brick is introduced between the antennas, the propagation mode changes from LOS to transmission mode, accompanied by a small amount of reflection and scattering paths. Considering these results, when the distance between them reaches 6 m, substrate penetration causes a decrease in transmission peak ratio compared to LOS peak to by approximately 15 dB while also introducing unstable multipath propagation. Path 2 represents a classic reflection path; however, it occasionally not a reflection path, but other scattering paths.

3.3 Indoor Assessment-Specific Analysis

In this section, a specific indoor scenario and corresponding channel characteristics are analyzed, including additional analysis of LOS, first and second order

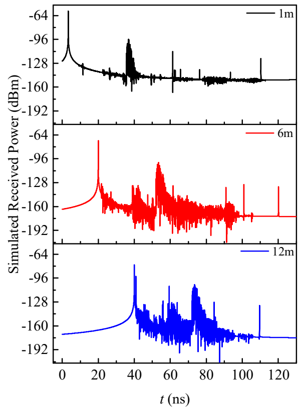

Figure 8. Compared ray-tracing results with different distance

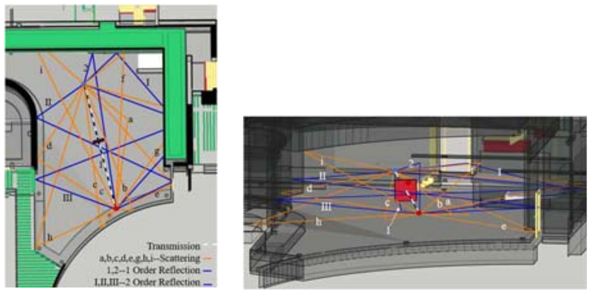

(a) (b)

Figure 9. (a) top view and (b) front view of the evaluated building and corresponding traces (Tx and Rx 12 m, and with brick)

Table 3. The summary of Paths in Figure 9

Path(m)	1	2	I	II	III	a	b
Path length(m)	12.3434	17.64	23.5448	25.2877	32.8553	14.0126	14.1864
τ (ns)	41.1446	58.8002	78.4828	84.2923	109.5177	46.7087	47.2881
Path(m)	c	d	e	f	g	h	i
Path length(m)	15.7346	16.8933	18.2842	19.2396	20.7873	23.8833	24.7067
τ (ns)	52.4486	56.3111	60.9473	64.1321	69.2909	79.6109	82.3555

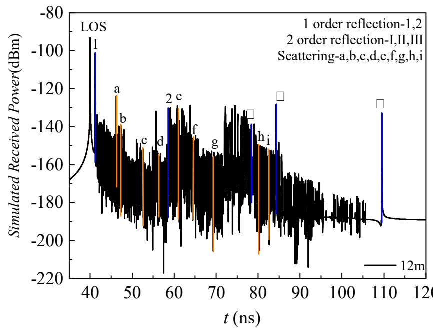

Figure 10. Ray-tracing simulated result-with brick

reflection paths, scattering paths and transmission path. Figure 8 illustrates the top view and front view of the evaluated building with a distance of 12 m between Tx and Rx antennas, along with the corresponding main radiation paths. The first-order reflection paths are denoted by Arabic numerals, while the second-order reflection paths are denoted by Roman numerals I, II, III. Lowercase letters represent scattering paths (Note that for convenience, scattering paths have been simplified to a single path instead of multiple paths; typically, they form a dense beam scattered on the wall). Table 2 presents specific path lengths and their corresponding time spectra. A more intuitive comparison is depicted in Figure 9 where the

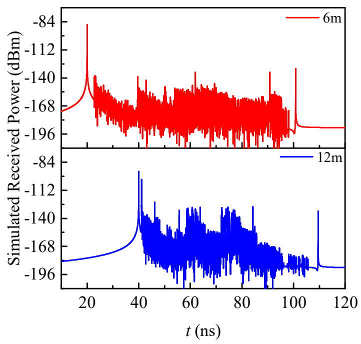

Figure 11. Compared ray-tracing results of different distance

nearest reflection path closely aligns with the LOS path, while scattering paths exhibit collective dispersion within a broad beam as evident from Figure 9. Second-order reflections primarily occur in the latter half of the time axis due to longer path lengths.

The simulation results in Figure 10 demonstrate the impact of varying distances (1 m, 6 m and 12 m) between the Tx and Rx antennas. It is evident that as the distance is decreased, there is a significant reduction in the number of scattering paths and a less pronounced presence of reflection paths.

For comparison, a simulation was also conducted for the scenario where bricks were placed midway between the Tx and Rx antennas in the LOS path. Taking a distance of 12 m between the Tx and Rx antennas as an example shown in Figure 11, Table 3 provides a summary of each path length and time spectra. A clear comparison chart is presented in Figure 12. In contrast to Figure 9, when obstructed by bricks, the LOS changes to transmission mode resulting in a significant drop in peak value, substantial increase in scattering paths, and similar trend with the without brick scenario observed for reflection paths.

The comparison results at various distances, as depicted in Figure 13, are consistent with the previously predicted trend. While multiple scattering paths exist for each antenna separations, reflection paths remain relatively stable across all cases.

4. Conclusion

In this study, our focus lies in modeling and simulating indoor channel scenarios within the 500 GHz – 750 GHz frequency band to gain a preliminary understanding of the channel characteristics in this frequency band. To validate the accuracy of our simulation platform, we compared its simulation results with measured data, demonstrating a strong agreement between the studies. During the simulation process, we employed horn antennas while and examined channel characteristics both with and without obstructions. By gradually increasing the distance between Tx and Rx antennas, we investigated channel behavior within the 500 GHz – 750 GHz frequency band.

Overall, our experimental results provide detailed data support regarding channel characteristics under different antenna types and environmental conditions, establishing a solid foundation for further research and applications.

6. Acknowledgements

The work was supported in part by the 2021–2025 National Measurement System Program of the U.K. Government's Department for Science, Innovation and Technology, under Science Theme Reference EMT24 of that Program and in part by the project (21NRM03 MEWS), which has received funding from the European Partnership on Metrology, co-financed from the European Union's Horizon Europe Research and Innovation Programme and by the Participating States. Funded by the European Union. Views and opinions expressed are however those of the author(s) only and do not necessarily reflect those of the European Union or EURAMET. Neither the European Union nor the granting authority can be held responsible for them.

References

[1]. D. He, K. Guan, D. Yan, H. Yi, Z. Zhang, X. Wang, Z. Zhong, N. Zorba, "Physics and AI-Based Digital Twin of Multi-Spectrum Propagation Characteristics for Communication and Sensing in 6G and Beyond," *IEEE Journal on Selected Areas in Communications*, **41**, 11, Nov. 2023, 3461-3473, doi: 10.1109/JSAC.2023.3310108.

[2]. X. Wang, K. Guan, D. He, Z. Zhang, H. Zhang, J. Dou, Z. Zhong, "Super-Resolution of Wireless Channel Characteristics: A Multitask Learning Model," *IEEE Transactions on Antennas and Propagation*, **71**, 10, Oct. 2023, 8197-8209, doi: 10.1109/TAP.2023.3305096.

[3]. H. Yi, K. Guan, P. Mathoipoulos, P. Xie, D. He, J. Dou, Z. Zhong, "Full-Wave Simulation and Scattering Modeling for Terahertz Communications," *IEEE Journal of Selected Topics in Signal Processing*, **17**, 4, July 2023, 713-728, doi: 10.1109/JSTSP.2023.3285099.

[4]. Y. Li, Y. Chen, D. Yan, K. Guan and C. Han, "Channel Characterization and Ray-Tracing Assisted Stochastic Modeling for Urban Vehicle-to-Infrastructure Terahertz Communications," *IEEE Transactions on Vehicular Technology*, **72**, 3, March 2023, 2748-2763, doi: 10.1109/TVT.2022.3217352.

[5]. K. Guan, D. He, B. Ai, Y. Chen, C. Han, B. Peng, Z. Zhong, T. Kürner, "Channel Characterization and Capacity Analysis for THz Communication Enabled Smart Rail Mobility," *IEEE Transactions on Vehicular Technology*, **70**, 5, May 2021, 4065-4080, doi: 10.1109/TVT.2021.3071242.

[6]. K. Guan , B. Peng, D. He, J. M, H. Yi, S. Rey, B. Ai, Z. Zhong, T. Kürner, "Channel Sounding and Ray Tracing for Intrawagon Scenario at mmWave and Sub-mmWave Bands," *IEEE Transactions on Antennas and Propagation,* **69**, 2, Feb. 2021, 1007-1019, doi: 10.1109/TAP.2020.3016399.

[10]. R. Piesiewicz, C. Jansen, S. Wietzke, D. Mittleman, M. Koch, T. Kürner. "Properties of Building and Plastic Materials in the THz Range". *Int J Infrared Milli Waves*, **28**, 363–371, March 2007. doi: 10.1007/s10762-007-9217-9.ss